Inventory of Supplemental Information

Supplemental Data: 6 Supplemental Figures and Legends
Supplemental Experimental Procedures
Supplemental Table Legends
Supplemental References

SUPPLEMENTAL DATA

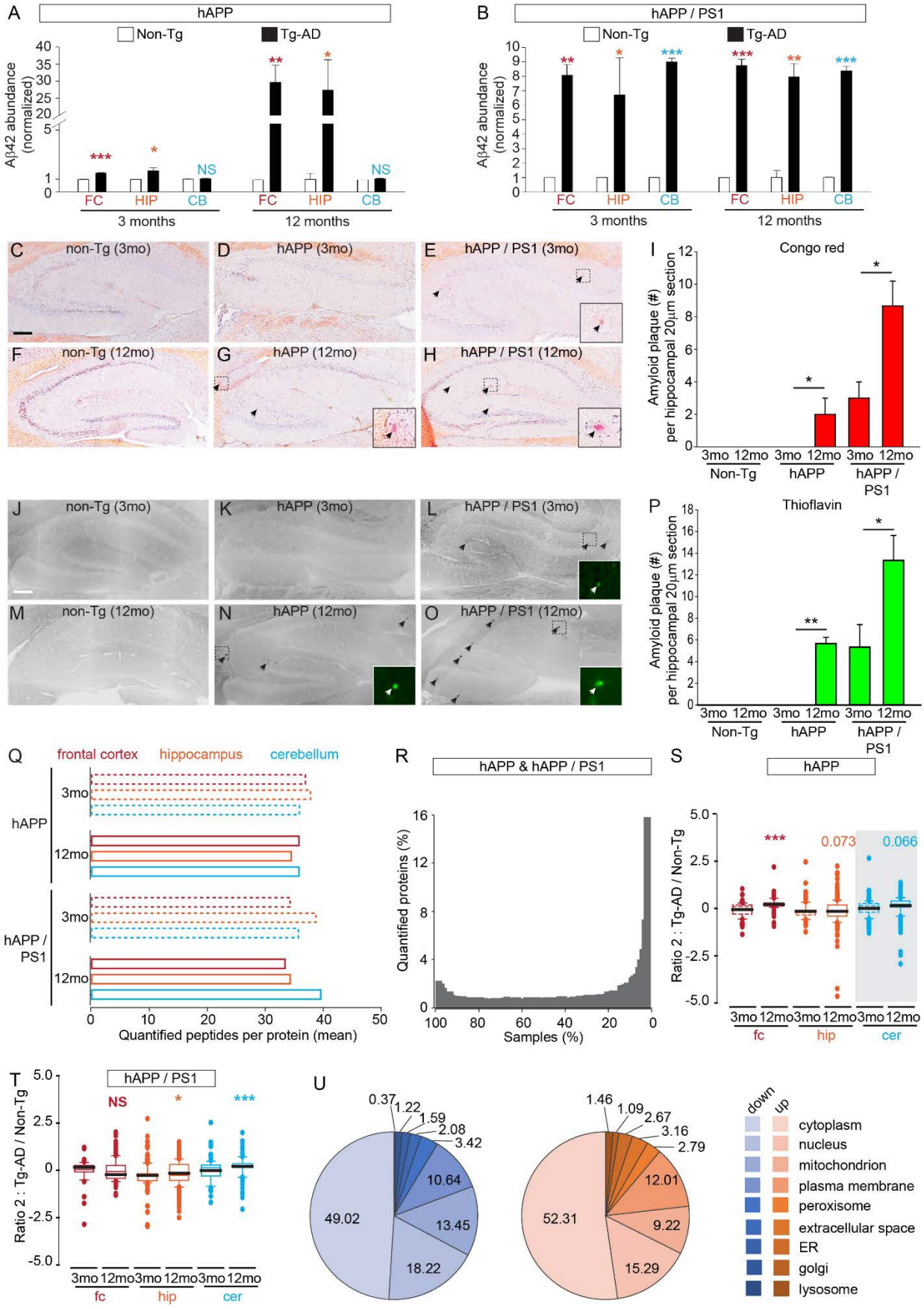

Figure S1 (related to Figure 1). Pathological assessment of the Tg-AD mice used for proteomic analysis (**A**) ELISA quantification of Aβ levels of the indicated hAPP mouse brain regions. For 3 months: Non-Tg frontal cortex (FC) = 1.000 ± 0.0247, hAPP FC = 1.502 ± 0.0375, Non-Tg hippocampus (Hip) = 1.000 ± 0.0113, hAPP Hip = 1.684 ± 0.220, Non-Tg cerebellum (Cer) = 1.000 ± 0.0405, hAPP Cer = 1.045 ± 0.0137. For 12 months: Non-Tg FC = 0.978 ± 0.0044, hAPP FC = 24.335 ± 4.958, Non-Tg Hip = 1.002 ± 0.476, hAPP Hip = 22.065 ± 8.740, Non-Tg Cer = 0.954 ± 0.0085, hAPP = 1.047± 0.0349; (**B**) Quantification of Aβ levels of the indicated hAPP / PS1 mouse brain regions by ELISA. For 3 months: Non-Tg FC = 1.000 ± 0.012, hAPP / PS1 FC = 7.950 ± 0.730, Non-Tg Hip = 1.000 ± 0.004, hAPP / PS1 Hip = 6.693 ± 2.538, Non-Tg Cer = 1.000 ± 0.006, hAPP / PS1 Cer = 8.905 ± 0.030. For 12 months: Non-Tg FC = 0.986 ± 0.002, hAPP / PS1 FC = 8.617 ± 0.431, Non-Tg Hip = 1.003 ± 0.483, hAPP / PS1 Hip = 7.926 ± 0.909, Non-Tg Cer = 1.013 ± 0.027, hAPP / PS1 Cer = 8.294 ± 0.039; (**C**-**H**) Congo red amyloid staining of sagittal brain slices showing the hippocampal region: (**C**) 3 month old Non-Tg; (**D**) 3 month old hAPP; (**E**) 3 month old hAPP / PS1; (**F**) 12 month old Non-Tg; (**G**) 12 month hAPP; (**H**) 12 month old hAPP / PS1; (**I**) Amyloid plaque quantitation indicating the visible number of plaques per hippocampal region from a 20 μm section; (**J**-**O**) Thioflavin S amyloid staining of sagittal brain slices showing the hippocampal region: (**J**) 3 month old Non-Tg; (**K**) 3 month old hAPP; (**L**) 3 month old hAPP / PS1; (**M**) 12 month old Non-Tg; (**N**) 12 month hAPP; (**O**) 12 month old hAPP / PS1; (**P**) Amyloid plaque quantitation indicating the visible number of plaques per hippocampal region from a 20 μm section. **(Q)** Average number of quantified peptides per protein used in the indicated model, brain region, and time point dataset. **(R)**The percentage of proteins quantified across all samples. **(S-T)** Summary box plot analysis for the significant protein (FDR-adjusted *p* value < 0.05) ratios for each of the indicated datasets. FC for hAPP but not hAPP / PS1, the difference between the average protein fold change between 3 and 12 months was significantly increased (-0.0621 ± 0.389 versus 0.214 ± 0.320; mean ± STD; *p* value = 1.34 E-8 by t test). For the HIP, we found a significant increase between 3 and 12 mo in hAPP / PS1 (-0.266 ± 0.619 versus -0.155 ± 0.604 mean ± STD; *p* value = 0.0240 by t test). For the CB we found a significant increase in the hAPP / PS1 model, (-0.00866 ± 0.554 versus 0.209 ± 0.489; mean + STD; *p* value = 3.34 E-4 by t test). Number of proteins (n) used at 3 and 12 mo time points are respectively for hAPP 138 and 162 for frontal cortex, 256 and 484 for hippocampus, 254 and 527 for cerebellum. **(U)** Proteome changes in subcellular compartments. Shown are the fractions of the proteome altered > 20% with *p* value < 0.05 by Student's t test from the total of down (blue) or up regulated (orange) proteins. Protein subcellular localization was predicted by MultiLoc2 (Blum et al., 2009). Scale bar (C & J) = 200 μm. Bar graphs show mean ± SD. **p* value < 0.05, ***p* value < 0.01, and ****p* value < 0.001 by Student's t test. n = 3 mice for each analysis.

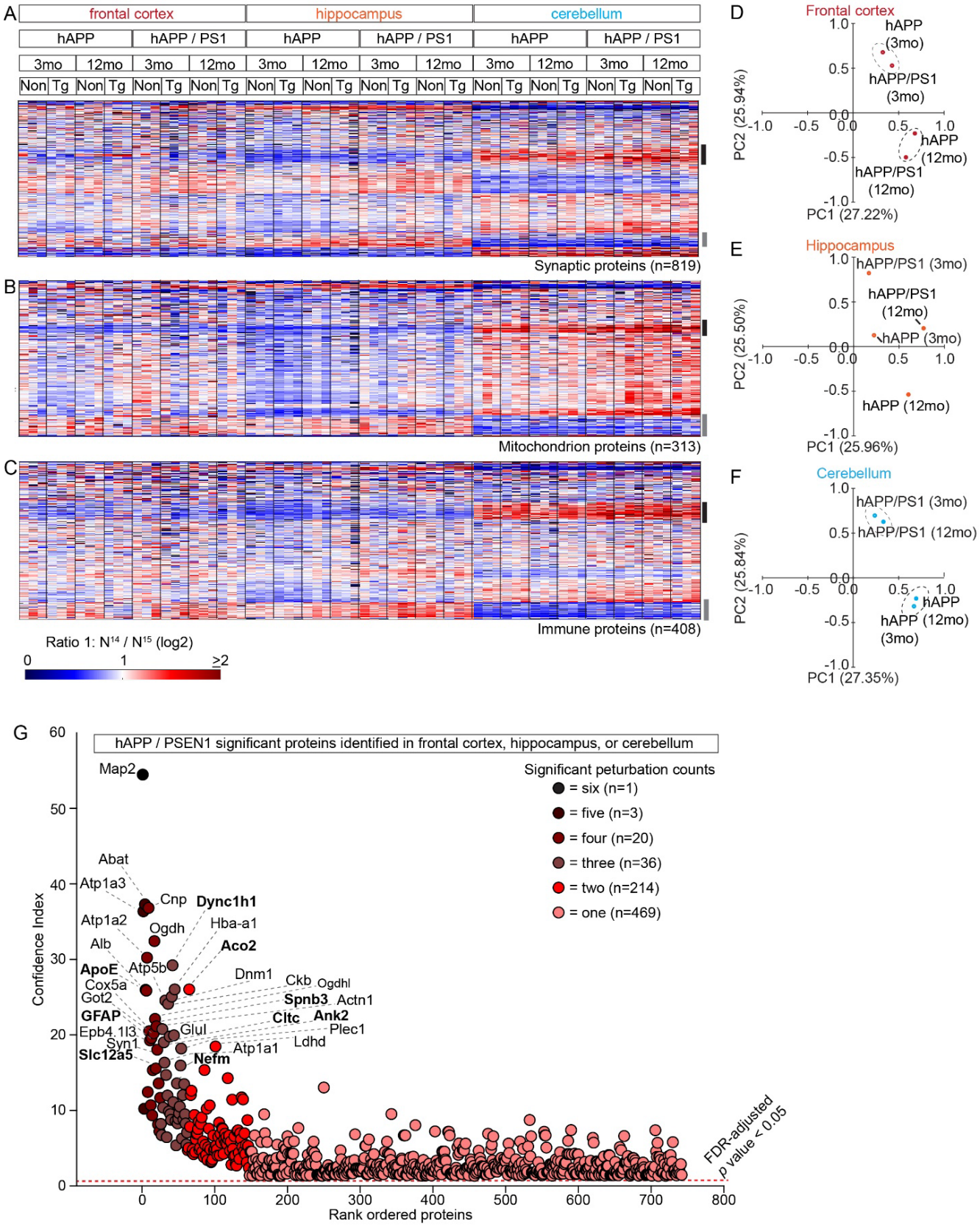

Figure S2 (related to Figure 3). Proteomic analysis of pre- and post-symptomatic Tg-AD mouse brains. **(A-C)** Heat maps depicting differential protein abundances after hierarchical clustering across sub-proteomes. For (A) synaptic proteins were

identified by the Genes to Cognition (G2C) database, for (B) mitochondrion proteins were identified by MitoCarta2.0, and for (C) immune proteins were identified by InnateDB. Missing values are indicated in black. **(D-F)** Principal component analysis of proteins in each analysis paradigm with *p* value < 0.05 by Student's t test shows brain region specific clustering. Frontal cortex proteomes (n = 1050 proteins) cluster based on age, cerebellum proteomes (n = 1207) cluster based on the Tg-AD model, while the hippocampal proteomes (n = 904 proteins) show less similarity. **(G)** Summary plot depicting the confidence index for all the significantly altered proteins in the hAPP / PS1 model. The number of datasets that each protein was identified in indicated by the shade of red. The ordering is based on the number of datasets that each protein was significantly altered (x-axis). Within each of those groups the proteins are arbitrarily ordered, and for visualization purposes only, *p* values were summed for those proteins identified as significant in multiple datasets (y-axis). Proteins with very small *p* values > 0 but < 3.42 E-09 were graphed as 1E-13 (see Tables S1-2), proteins found in the top 30 proteins in both models are indicated in bold.

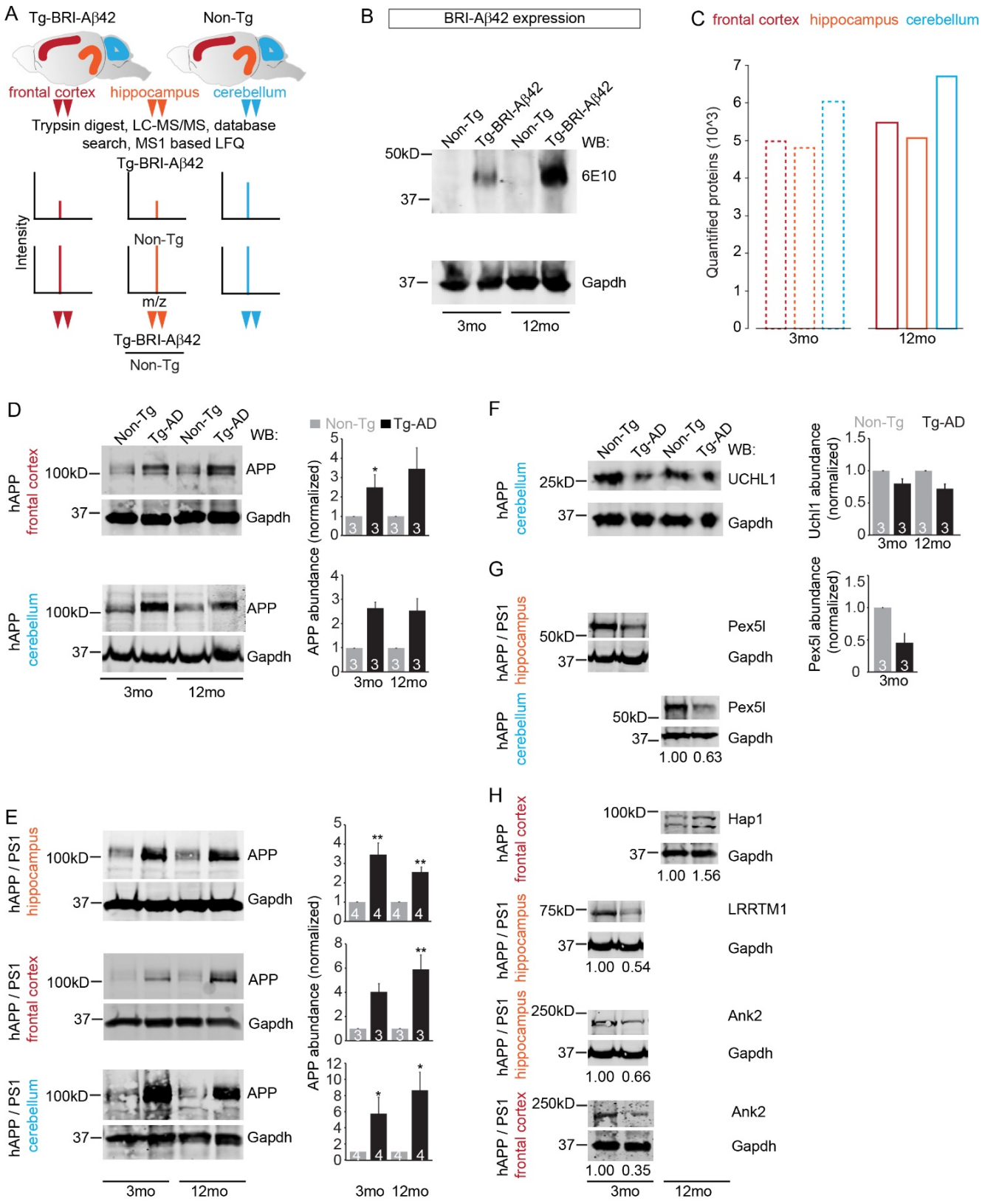

Figure S3 (related to Figure 3). Confirmation of MS results **(A)** Experimental design and analysis work flow. Frontal cortex, hippocampus, and cerebellum were dissected from 3 and 12 mo old BRI-Aβ42 or non-Tg litter mates. Proteins were digested into peptides and analyzed by single shot MS based proteomics and bioinformatics. The protein ratio is calculated is determined relative to the control animals. **(B)** Representative WB analysis of cerebellum extracts from 3 and 12 mo old BRI-Aβ42 or non-Tg litter mates showing increased expression of BRI-Aβ42 fusion protein without an increase in APP

levels. **(C)** Summary of the number of quantified proteins in our 6 datasets. We quantified more than 4,000 proteins in each analysis. n = 4 mice per condition. **(D)** Western blot analysis of APP in hAPP mouse brains at 3 and 12 mo and quantification. **(E)** Western blot analysis of APP in hAPP / PS1 mouse brains at 3 and 12 mo and quantification. **(F)** Western blot analysis and quantification of Uchl1 in hAPP cerebellum at 3 and 12 months. **(G)** Western blot analysis and quantification of Pex5l in hAPP / PS1 hippocampus at 3 months. Western blot analysis of Pex5l in hAPP cerebellum at 12 months. n = 2. **(H)** Western blot analysis of HAP1 in hAPP in frontal cortex at 12 mo. n = 1. Western blot analysis of LRRTM1 in hAPP / PS1 hippocampus at 3 mo. n = 2. Western blot analysis of Ank2 in hAPP / PS1 hippocampus at 3 months. n = 2, and in hAPP / PS1 frontal cortex at 3 mo. n = 1. * p value < 0.05; ** p value < 0.01 by Student's t test. Bar graphs (B, D, F, H, J, and L) show mean ± SEM; number in bars indicates biological replicates for each condition.

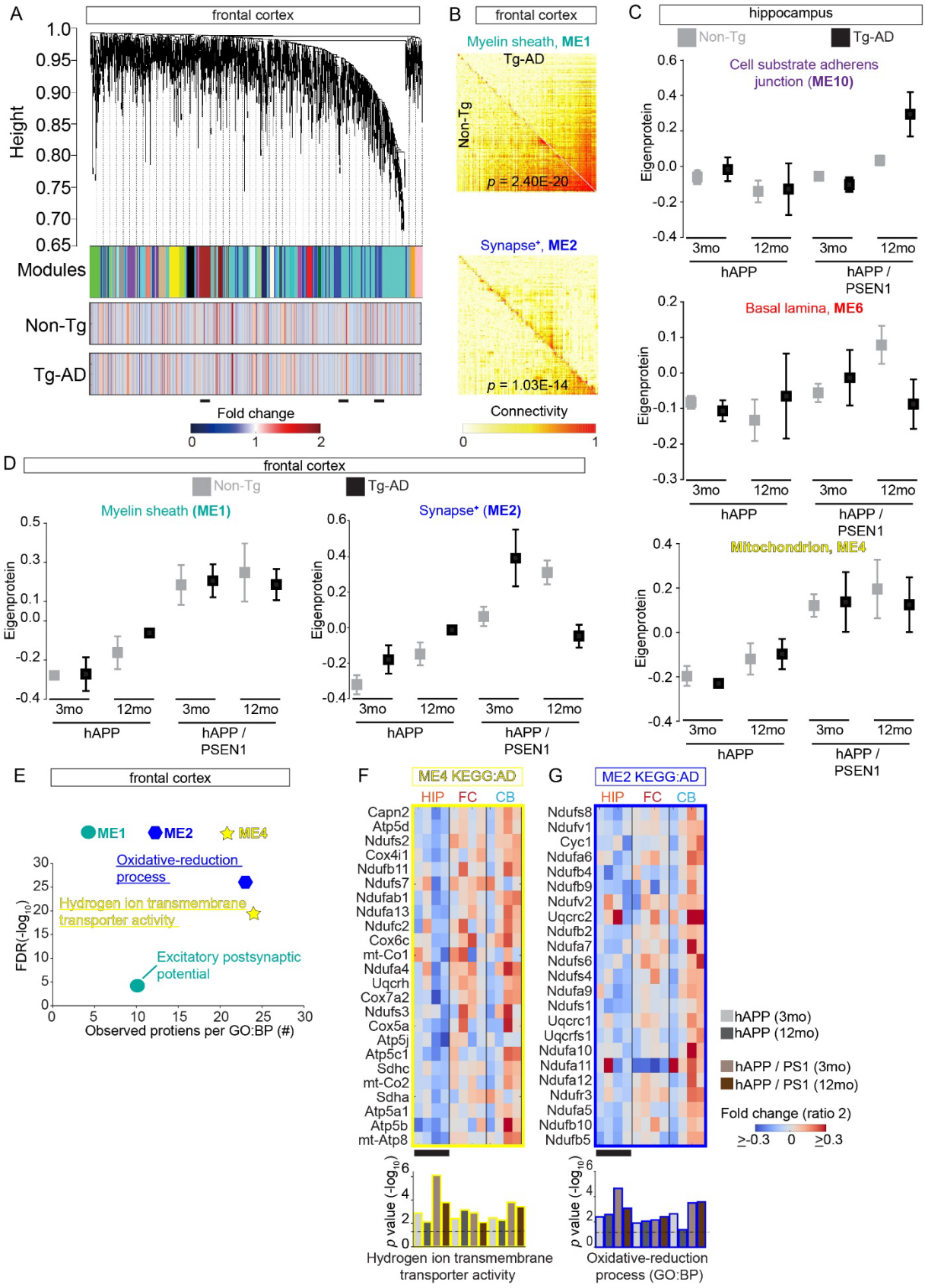

Figure S4 (related to Figure 4). Protein co-expression network analysis of Tg-AD brains **(A)** FC protein clustering trees from pooled data from both Tg-AD models and time points. Each module (cluster) is indicated by a distinct non-grey color

just below the tree and grey represents proteins unassigned to an ME. The two rows of heat maps below show the association of individual proteins with Q for non-Tg or Tg-AD groups. Blue and red shading indicates proteins with reduced or increased expression, respectively, with increasing Q. Black bars indicate protein groups with differential expression. **(B)** Individual topological overlap matrices of differentially connected modules in FC of both Tg-AD models. Module assignment based on the most significant GO assignment, (except ME2 see Table S4). Adjusted global *p* values shown are calculated from meta-analysis based on pooled associations. Shown are all modules with $p < 1$ E-4. **(C-D)** Summary expression value (eigenprotein) and hypergeometric enrichment *p* values of HIP (C) and FC (D) for the indicated module, time point, and model. Non-Tg is in grey and Tg-AD in black. **(E)** Gene ontology enrichment analysis for the frontal cortex proteins belonging to ME1 (turquoise), ME2 (blue), ME9 (magenta), ME12 (greenyellow). Scatter plot shows the number of proteins in each ontology (y-axis) versus corrected *p* value (x-axis) and includes each assignment with the highly significant ontologies labeled and the most significant underlined. **(F-G)** Protein expression matrix (ratio 2 see figure 1) for the indicated modules and enrichment analysis for both Tg-AD models and time points. Black bars indicate the hippocampal datasets which show contrasting protein expression patterns. Below is bar graph based on the hypergeometric enrichment *p* values for each data set (brain region, model, and time point), and dotted line indicates an adjusted $p < 0.05$.

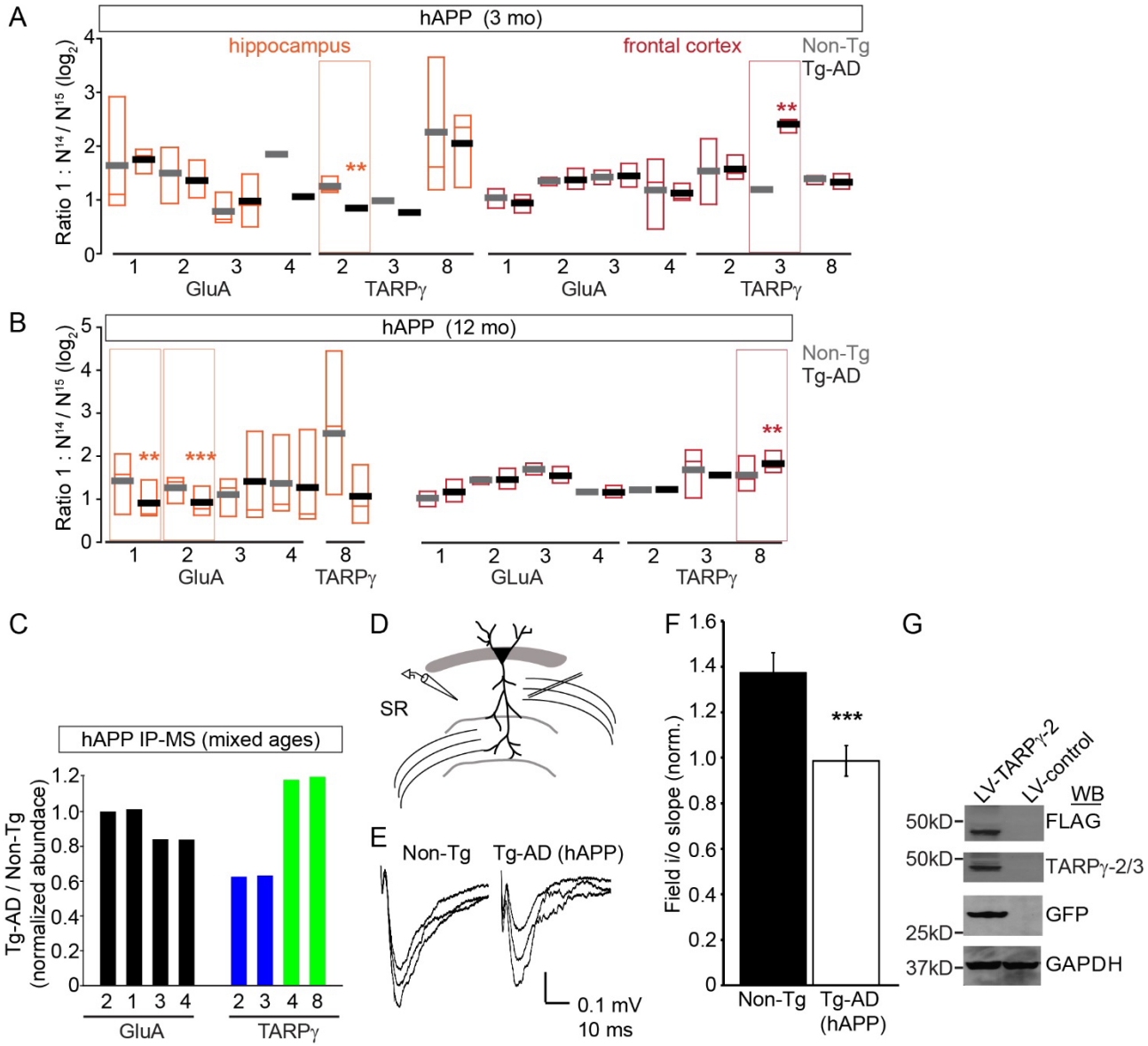

Figure S5 (related to Figure 6). Analysis of AMPARs in hAPP mice **(A and B)** Extracted quantitative proteomic data from 3 and 12 mo datasets of AMPARs including GLuA1-4 core subunits and TARP axillary subunits in hAPP hippocampus and frontal cortex. (A) For the hippocampus at 3 mo TARPγ-2 is the only AMPAR protein with significantly altered levels (Non-Tg = 1.25 ± 0.162, Tg-AD = 0.85 ± 0.0230, n = 3 biological replicates; *p* value = 0.00423 by Student's t test and 0.0840 FDR-adjusted *p* value. (B) For the frontal cortex at 3 mo TARPγ-3 is the only AMPAR protein with significantly altered levels (Non-Tg = 1.165 ± 0.139, Tg-AD = 2.38 ± 0.0353, n = 3 biological replicates; *p* value = 7.21 E-4 by Student's t test and 0.0348 FDR-adjusted *p* value. **(C)** Representative mass spectrometry analysis of AMPARs with anti-GluA2 antibodies based on the number of MS / MS spectral counts and normalized to GluA2. **(D)** Schematic of field recording in CA1. Stimulating and recording electrodes were placed in stratum radiatum of either non-TG or hAPP Tg-AD littermates. **(E)** Example field recordings from non-TG or Tg-AD hAPP-J9 animals aged 3 mo demonstrating the field response of three different stimulation intensities. **(F)** Quantification of field slope normalized to fiber volley amplitude (Non-Tg: 1.37 ± 0.08, n = 28; Tg-AD: 0.98 ± 0.06, n = 22; *p* value < 0.001, Student's t test). **(G)** Western blot analysis of HEK293 cells transfected with lenti viral DNA expressing TARPγ–2-Flag-IRES-GFP or vector with anti-Flag, anti-TARPγ–2/3, anti-GFP, or anti-GAPDH antibodies. **p* value < 0.05, ***p* value < 0.01, and ****p* value < 0.001 by Student's t test.

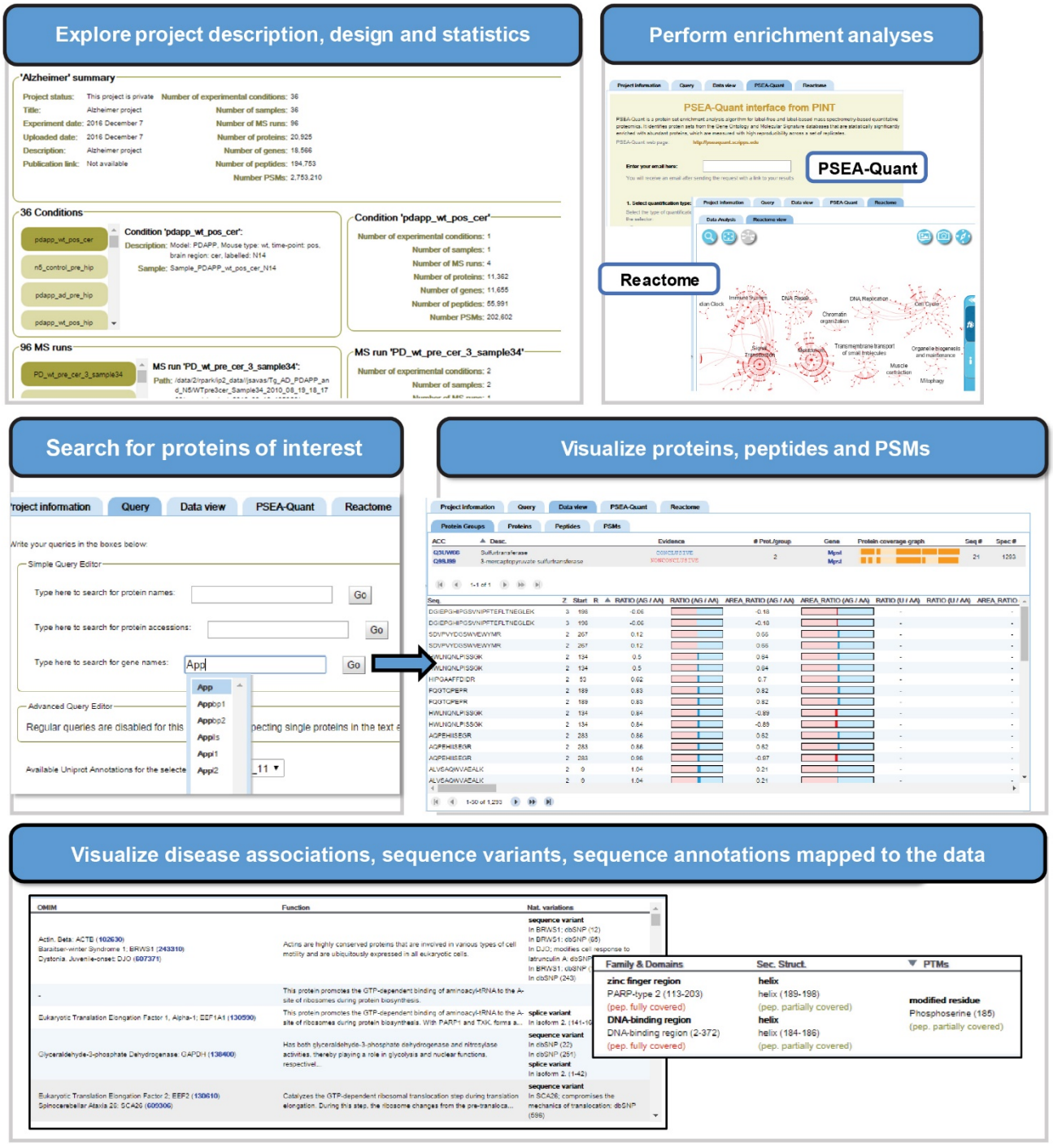

Figure S6 (related to Figure 1). Project visualization in PINT (Proteomics INTegrator) This project has been uploaded to the TSRI's PINT server located at http://sealion.scripps.edu/pint. Project metadata and experimental design can be explored and specific proteins or genes can be searched. Resulting experimental proteomics data, including quantitative information is shown in different tables and is automatically mapped to UniProtKB annotations (disease associations, sequence variants, sequence annotations., etc.). PINT also provides annotation enrichment analysis tools, such as PSEA-Quant (Lavallee-Adam et al., 2014) and Reactome (Fabregat et al., 2016).

SUPPLEMENTAL EXPERIMENTAL PROCEDURES

Animal breeding, husbandry, metabolic nitrogen-15 labeling, and transgenic AD mouse models
All animal procedures were approved by Institutional Animal Care and Use Committee of the University of California, San Diego, The Salk Institute, and The Scripps Research Institute. TSRI IACUC / Department of Animal Resources (approved protocol number 07-0083) and UCSD Institutional Animal Care and Use Committee (IACUC) (approved protocol numbers S03154, S03155, S02216M). For euthanasia, mice were anesthetized with isoflurane and decapitated. Ten C57BL6 female mice were metabolically labelled with ^{15}N-rich, Spirulina-based diet (Cambridge Isotopes and Harlan Laboratories) for 12 weeks starting at P21 (Wu et al., 2004) . The ^{15}N protein enrichment in brain, was determined to be approximately 90-95% (MacCoss et al., 2005). For the PDAPP model we used the less aggressive J9 line, except for the AMPAr immunoprecipitation – mass spectrometry / western blots and whole cell electrophysiology in which out of necessity we used J20 mice (RRID:IMSR_JAX:004662) (Mucke et al., 2000). All PDAPP-J9 (hAPP) mice on C3H/B6 background were female, 3mo = 3.6 - 3.8mo and 12mo = 12.3 – 13.6 mo. PDAPP-J20 mice were mostly female and ranged in age from 3 – 12 mo. For hAPP / PS1 mice (B6C3-Tg(APPswe,PSEN1dE9)85Dbo/Mmjax– 129x1/SvJ) (RRID:MMRRC_037564-JAX), all were female and 3 mo = 3.0 – 3.6 mo and 12 mo = 12.3 – 15.0 mo (Borchelt et al., 1996; Cohen et al., 2009). For BRI-Aβ42 mice (C57BL/6J background), most mice were female, 3 mo = 3.0 – 3.2 mo and 12 mo = 12.2 – 12.9 mo (RRID:IMSR_JAX:007182) (McGowan et al., 2005). All genotyping was verified by multiple PCR reactions. All hAPP, hAPP / PS1, and BRI-Aβ42 mice used were heterozygous for the transgenes.

Preparation of protein extracts from mouse brains
Mice were euthanized with isoflurane followed by acute decapitation. Brains were extracted and split into two hemispheres, one for proteomic analysis / ELISA and the other for histology (described below). The hippocampus, frontal cortex, and cerebellum were immediately dissected in pH 7.4 PBS (cat. #: 10010031, Thermo) and flash frozen in liquid nitrogen. Brain regions were then homogenized with a micro douce homogenizer (100 µl for hippocampus, 200 µl for cerebellum, and 500 µl for frontal cortex) in 4 mM HEPES, 0.32 M sucrose with protease inhibitors (EDTA-free cOmplete Protease Inhibitor Tablets, Roche). Protein extracts were diluted in homogenization buffer and protein concentration was determined by BCA assay (cat. #: 23225, Thermo). For PDAPP-J9 and APPswe, PSEN1dE9, fifty µg of protein of each Tg-AD or non-Tg litter mate was mixed 1:1 with ^{15}N labeled whole brain homogenate and a total of 100 µg of sample was further processed together in the same tube. For BRI-Aβ42 mice, 50 µg of protein was processed without mixing with ^{15}N. Solid urea was added to the extract to reach a final concentration of 8M and subsequently processed with ProteasMAX (cat. #: V2072, Promega) following the manufacturer's instructions. The samples subsequently were reduced by 5 mM Tris(2 carboxyethyl)phosphine at room temperature for 20 min, alkylated in the dark by 10 mM iodoacetamide for 20 min, and digested with sequencing grade modified trypsin (cat. #: V5117, Promega) overnight at 37 °C, and the reaction was stopped by acidification.

Amyloid plaque staining, Aβ42 Enzyme-Linked Immunosorbent Assay (ELISA) assays, and Western blotting
Mouse sagittal brain hemispheres were fixed in 4% paraformaldehyde. Brains were then cryoprotected for 24 hours in 30% sucrose. Brain hemispheres were then transferred to O.C.T. in cryomolds and flash frozen on dry ice. Cryosections were prepared at 20µm and stained with thioflavin S or Congo red / haematoxylin and eosin by standard procedures (Ly et al., 2011). Sections were mounted and imaged with a TissueGnostics system with a 10X objective. Human Beta Amyloid [1-42] ELISA was performed with 200-500 µg of mouse brain region homogenate as input prepared with 8 M guanidine. We used synthetic Aβ42 peptide standards as performed the assay described by the ELISA kit manufacturer (Cat. #: KHB3441, Thermo). Fifty micrograms of brain region homogenate (same animals used for MS analysis) was diluted in sample buffer and separated by SDS-PAGE. Antibodies used for western blot analysis are as follows: anti-Amyloid Precursor Protein (APP) CTF at 1:1000, immunogen is synthetic peptide from the C-terminal 15 residues of APP (aa 680-695) rabbit polyclonal (CT15) reacts with human and mouse APP (Soriano et al., 2001), anti-HAP1 purified mouse monoclonal at 1:1000 (BD Biosciences Cat# 611302 RRID:AB_398828), anti-GAPDH rabbit monoclonal at 1:1000 (Cell Signaling Technology Cat# 2118 RRID:AB_561053), anti-UCHL1 rabbit polyclonal at 1:1000 (Proteintech Group Cat# 14730-1-AP RRID:AB_2210497), anti-Pex5l mouse monoclonal at 1:1000 (UC Davis/NIH NeuroMab Facility Cat# 75-245 RRID:AB_10673515), anti-Ankyrin B rabbit polyclonal at 1:500 (Santa Cruz Biotechnology Cat# sc-28560 RRID:AB_2242828), anti-LRRTM1 sheep polyclonal at 1:1000 (R and D Systems Cat# AF4897 RRID:AB_10643427).

Orbitrap Velos and Fusion mass spectrometry analysis
The protein digest was pressure-loaded into a 250 µm i.d capillary packed with 2.5 cm of 10 µm Jupiter C18 resin (Phenomenex) followed by an additional 2.5 cm of 5 µm Partisphere strong cation exchanger (Whatman)(Link et al., 1999; Savas et al., 2014; Washburn et al., 2001). The column was washed with buffer containing 95 % water, 5 % acetonitrile, and 0.1 % formic acid. After washing, a 100 µm i.d capillary with a 5 µm pulled tip packed with 15 cm of 4 µm Jupiter C18

resin (Phenomenex) was attached to the filter union and the entire split-column (desalting column–union–analytical column) was placed in line with an Agilent 1200 quaternary HPLC and analyzed using a modified 11 step separation described previously (Savas et al., 2012). The buffer solutions used were 5 % acetonitrile / 0.1 % formic acid (buffer A), 80 % acetonitrile / 0.1 % formic acid (buffer B), and 500 mM ammonium acetate / 5 % acetonitrile / 0.1 % formic acid (buffer C). The ^{15}N mass spectrometry (MS) analysis was performed on high resolution LTQ Velos Orbitrap mass spectrometer (Thermo) as follows. Step 1 consisted of a 90 min gradient from 0-100 % buffer B. Steps 2-11 had a similar profile with the following changes: 5 min in 100% buffer A, 3 min in X% buffer C, a 10 min gradient from 0-15 % buffer B, and a 108 min gradient from 15-100 % buffer B. The 3-min buffer C percentages (X) were 10, 20, 30, 40, 50, 60, 70, 80, 90, 100 %, respectively for the 11 step analysis. As peptides eluted from the microcapillary column, they were electrosprayed directly into the MS with the application of a distal 2.4 kV spray voltage. A cycle of one full-scan mass spectrum (400-1800 m/z) at a resolution of 60,000 followed by 15 data dependent MS/MS spectra at a 35% normalized collision energy was repeated continuously throughout each step of the multidimensional separation. Maximum ion accumulation times were set to 500 ms for survey MS scans and to 100 ms for MS2 scans. Charge state rejection was set to omit singly charged ion species and ions for which a charge state could not be determined for MS/MS. Minimal signal for fragmentation was set to 1,000. Dynamic exclusion was enabled with a repeat count: 1, duration: 20.00 S, list size: 300, exclusion duration 30.00 S, exclusion mass with high/low: 1.5 m/z. Application of mass spectrometer scan functions and HPLC solvent gradients were controlled by the Xcalibur data system.

For OT Fusion Tribrid MS analysis of BRI-Aβ42 brain tissue extracts, the tryptic peptides were purified with Pierce C18 spin columns (Thermo). Three micrograms was auto-sampler loaded with a Thermo EASY nLC 1000 UPLC pump onto a vented Acclaim Pepmap 100, 75 um x 2 cm, nanoViper trap column coupled to a nanoViper analytical column (cat.#: 164570, Thermo, 3 µm, 100 Å, C18, 0.075 mm, 500 mm) with stainless steel emitter tip assembled on the Nanospray Flex Ion Source with a spray voltage of 2000 V. Buffer A contained 94.785% H_2O with 5% ACN and 0.125% FA, and buffer B contained 99.875% ACN with 0.125% FA. The chromatographic run was for 4 hours in total with the following profile: 0-7% for 7, 10% for 6, 25% for 160, 33% for 40, 50% for 7, 95% for 5 and again 95% for 15 minutes receptively. Additional MS parameters include: Ion transfer tube temp = 300 °C, Easy-IC internal mass calibration, default charge state = 2 and cycle time = 3 s. Detector type set to Orbitrap, with 60K resolution, with wide quad isolation, mass range = normal, scan range = 300-1500 m/z, max injection time = 50 ms, AGC target = 200,000, microscans = 1, S-lens RF level = 60, without source fragmentation, and datatype = positive and centroid. MIPS was set as on, included charge states = 2-6 (reject unassigned). Dynamic exclusion enabled with n = 1 for 30 s and 45 s exclusion duration at 10 ppm for high and low. Precursor selection decision = most intense, top 20, isolation window = 1.6, scan range = auto normal, first mass = 110, collision energy 30%, CID, Detector type = ion trap, OT resolution = 30K, IT scan rate = rapid, max injection time = 75 ms, AGC target = 10,000, Q=0.25, inject ions for all available parallelizable time.

Analysis of Tandem Mass Spectra

Protein identification and quantification and analysis were done with Integrated Proteomics Pipeline - IP2 (Integrated Proteomics Applications, Inc., San Diego, CA. http://www.integratedproteomics.com/) using ProLuCID, DTASelect2, Census, and QuantCompare. Spectrum raw files were extracted into ms1 and ms2 files using RawExtract 1.9.9 (http://fields.scripps.edu/downloads.php), and the tandem mass spectra were searched against EBI IPI mouse protein databases (http://www.ebi.ac.uk/IPI/IPImouse.html, downloaded on January 1, 2009)(McDonald et al., 2004). Since we work with brain tissue which has many cell types and mRNA alternative splicing we chose large databases to maximize our analysis potential. All the peptide identifications have been mapped to genes and the details can be found in our online database where all proteins were also mapped to UniprotKB accessions. To estimate peptide FDRs accurately, we used a target/decoy database containing the reversed sequences of all the proteins appended to the target database (Elias and Gygi, 2007). Tandem mass spectra were matched to sequences using the ProLuCID algorithm with 50 ppm peptide mass tolerance for precursor ions and 400 ppm for fragment ions (Xu et al., 2015).

ProLuCID searches were done on an Intel Xeon cluster running under the Linux operating system. The search space included all fully and half-tryptic peptide candidates that fell within the mass tolerance window with no miscleavage constraint. Carbamidomethylation (+57.02146 Da) of cysteine was considered as a static modification. The validity of peptide/spectrum matches (PSMs) was assessed in DTASelect2 (using two SEQUEST-defined parameters, the cross-correlation score (XCorr), and normalized difference in cross-correlation scores (DeltaCN) (Cociorva et al., 2007; Eng et al., 1994; Tabb et al., 2002). The search results were grouped by charge state (+1, +2, +3, and greater than +3) and tryptic status (fully tryptic, half-tryptic, and nontryptic), resulting in 12 distinct subgroups. In each of these subgroups, the distribution of Xcorr, DeltaCN, and DeltaMass values for (a) direct and (b) decoy database PSMs was obtained; then the direct and decoy subsets were separated by discriminant analysis. Full separation of the direct and decoy PSM subsets is not generally possible; therefore, peptide match probabilities were calculated based on a nonparametric fit of the direct and decoy score distributions.

A peptide confidence of 0.95 was set as the minimum threshold. The FDR was calculated as the percentage of reverse decoy PSMs among all the PSMs that passed the confidence threshold. Each protein identified was required to have a

minimum of one half-tryptic peptide; however, this peptide had to be an excellent match with an FDR less than 0.001 and at least one excellent peptide match. After this last filtering step, protein FDRs were below 1% for each sample analysis based on decoy hits.

Each dataset was searched twice, once against light and then against heavy protein databases. After the results from ProLuCID were filtered using DTASelect2, ion chromatograms were generated using an updated version of a program previously written in our laboratory (MacCoss et al., 2003). This software, called "Census" (Park et al., 2008a), is available from the authors for individual use and evaluation through an Institutional Software Transfer Agreement (see http://fields.scripps.edu/census for details). First, the elemental compositions and corresponding isotopic distributions for both the unlabeled and labeled peptides were calculated, and used to determine the appropriate m/z range from which to extract ion intensities, which included all isotopes with greater than 5 % of the calculated isotope cluster base peak abundance. MS1 files were used to generate chromatograms from the m/z range surrounding both the unlabeled and labeled precursor peptides. Census calculates peptide ion intensity ratios for each pair of extracted ion chromatograms. The core of the program is a linear least-squares correlation that is used to calculate the ratio (i.e., slope of the line) and closeness of fit [i.e., correlation coefficient (r)] between the data points of the unlabeled and labeled ion chromatograms. Census allows users to filter peptide ratio measurements based on a correlation threshold; the correlation coefficient (values range form 0-1) represents the quality of the correlation between the unlabeled and labeled chromatograms and can be used to filter out poor-quality measurements. In this study, only peptide ratios with the coefficient correlation values (r^2) greater than 0.5 were used for further analysis. In addition, Census provides an automated method for detecting and removing statistical outliers. In brief, SDs are calculated for all proteins using their respective peptide ratio measurements. The Grubbs test (p value < 0.01) is then applied to remove outlier peptides. The outlier algorithm is used only when more than two peptides are found in the same protein, because the algorithm becomes unreliable for a small number of measurements. Final protein ratios were generated with QuantCompare, which uses Log two-fold change on the biological replicates. The statistical significance labeled of the differential expression of all proteins was assessed using a two-tailed one-sample *t*-test on their corresponding peptide quantification ratios between both conditions. The obtained p values were FDR-adjusted for multiple hypothesis testing using the Benjamini–Hochberg correction (Benjamini and Hochberg, 1995). Proteins with FDR-adjusted p values < 0.05 and for which quantification measurements were obtained in at least two biological replicates in both conditions were considered for further analyses.

We performed label-free quantitative analysis using Census through Integrated Proteomics Pipeline (IP2)(Park et al., 2008b). We grouped biological replicates of each sample to determine the protein level. Census used protein identification results from DTASelect2 (Cociorva et al., 2007; Tabb et al., 2002) and generated a reconstructed MS1 based chromatogram for each identified peptide. When peptides are not identified in all the relevant samples, Census went through spectra searching them using accurate precursor mass, retention time, and charge states in order to retrieve them to build chromatograms. To increase accuracy for finding peptide precursors, we calculated Pearson product-moment correlation coefficient comparing theoretical and experimental isotope distributions to minimize false peak detection. Peak area of each peptide was normalized by using ion injection time. When peaks are not detected, we calculated background noise to assign small values to peptides. We calculated protein abundance from average of peptide intensities. The statistical significance label free of the differential expression of all proteins was assessed using a two-tailed paired *t*-test on their corresponding peptide quantification ratios between both conditions. Similar to labeled analysis, FDR-adjusted p values are calculated using the Benjamini–Hochberg correction.

Statistical analyses, heat maps, principal component analysis (PCA), bioinformatic analysis of subcellular compartments, and literature search

For all heat maps, we used 3 biological replicates for each experimental group, required each protein to be quantified in a minimum of 57 (out of a total of 72) datasets and had to be quantified in each brain region. We used the Genes to Cognition protein database (http://www.genes2cognition.org) to identify synaptic proteins, MitoCarta2.0 for mitochondrial proteins (http://www.broadinstitute.org/files/shared/metabolism/mitocarta/mouse.mitocarta.2.0.html), and InnateDB (http://www.innatedb.com/basicSearch.do) to identify the immunological proteins. Missing values are shown in black. For PCA, we used XLSTAT software and require the included proteins to be quantified with p value < 0.05 by t-test in at least one analysis paradigm and we inserted a value of 0 for any missing values. To investigate the subcellular compartment(s) which the perturbed proteins localize we used the subcellular protein localization prediction system Multiloc2. We removed all redundant proteins and required proteins to have a p value < 0.05 by t test and $\geq$ 20 % change in abundance in at least one dataset to be consider for Multiloc2 (Blum et al., 2009).

Box plots define 25th and 75th percentile and statistical analysis were performed with student's t-test with 2 tails and un-equal variance. For quantification of APP levels, only peptide sequences with 100 % homology between human and mouse were used. Bar graphs (Figure S1) show mean ± SD with student's t test with 1 tail and un-equal variance (A & B) with 2 tails and equal variance (I & P). Bar graphs for human AMPAR purifications with MS analysis, statistics were performed with Student's t test with 1 tail and 2 sample equal variance (Figure 6B). Western blot quantification Bar graphs (Figure S3) show mean ± SEM and student's t test with 1 tail and two-sample equal variance. We used the program 'Venn

Diagram Plotter' to construct two and three circle Venn diagrams (aka Euler diagrams) that was developed at the PNNL (OMICS.PNL.GOV). For Figure 3B, only peptides with 100% sequence homology between mouse and human were included.

For Figure 3A and S2G, for visualization purposes only, we generated protein "confidence plots". To construct these figure panels, first we grouped the proteins based on the number of datasets (model, brain region, age) they were found significantly altered (indicated by the color shading). For Figure 3A there were four groups (proteins significantly altered in four, three, two, or one dataset) and similarly for Figure S2G there were six groups (proteins significantly altered in six, five, four, three, two, or one dataset). These groups were then rank ordered from high to low (x-axis). Within each of these groups, the proteins were arbitrary ordered. For each protein, we transposed the *p* values based on –log10 transposed (y-axis). For proteins found significantly altered in multiple datasets, we summed the transposed p values for visualization purposes.

For every protein, we identified as being altered in the hippocampus or frontal cortex in both models (Table S5) we investigated if they had previously been found linked to AD. We first searched on Pubmed and Web of Science for any earlier publications using the same basic query for both databases (TS=[protein] AND TS=Alzheimer NOT TS=Review).We used genecards and uniprot supplement and for potential protein / gene aliases.

Weighted gene / protein co-expression network analysis (WGCNA)

The consensus weighted correlation networks were constructed across both non-Tg and Tg-AD groups for each brain regions with free R software package (Langfelder and Horvath, 2008; Zhang and Horvath, 2005). The specific datasets for each analysis is as follows (dataset numbers correspond to the numbering indicated in Table S6): FC = 137-9, 124-7, 89-92, 77-9, 112-6, 101-3, 65-7, 53-7. HIP = 140-4, 128-31, 93-5, 80-4, 117-9, 104-8, 68-72, 58-61. All groups consisted of three biological replicates except 3 m hAPP non-Tg FC that had two biological repeats and one technical repeat. Briefly, before the analysis, protein IDs with 14 or more missing values were filtered out, resulting in three pairs of datasets: 1912 protein IDs for hippocampus groups, 2146 protein IDs for frontal cortex groups and 2169 protein IDs for cerebellum groups. The soft power threshold was set to 12 for hippocampus groups, 6 for frontal cortex groups to arrive at the network adjacency. For the cerebellum groups, we failed to form a scale free consensus network which may due to a low noise/signal ratio. The power transformation set adjacency of negatively correlated proteins to zero and suppressed adjacency of weakly correlated proteins (due to noise) to nearly zero. The adjacency of positively correlated proteins is positive. Consensus modules and modules eigengenes were calculated with free R software package as described before (Langfelder et al., 2016). Briefly, consensus modules were identified using consensus dissimilarity-based clustering procedure (Langfelder et al., 2016), and consensus module eigengenes represented a summary expression profile for all the proteins in each consensus modules. We used the built-in R function GOenrichmentAnalysis and STRING 10.0 (www.string-db.org) functions to calculate the Gene Ontology (GO) terms enrichments and false discovery rate (FDR) for each consensus module (von Mering et al., 2005). To test if any of our MEs are significantly enriched for the proteins involved with AD we used the KEGG AD pathway (hsa05010) as a reference.

Consensus module membership: For each consensus module, we calculated the Pearson coefficient between the eignegene and expression profile of each protein in this module (Langfelder et al., 2016). The values ranged from -1 to 1. For each protein, there were two values, one for Non-Tg and one for Tg-AD dataset. Then we used meta-analysis to summarize these two values into a single meta-analysis Z statistic (Langfelder et al., 2016; Zaykin, 2011). A protein with higher value indicated that its expression profile was more similar to the summary profile of this module. We defined the top 50 proteins with highest values as hub proteins, which represented the summarized expression profile for the whole module. The hub proteins networks were constructed based on the power transformed adjacency using Cytoscape v. 3.1.0 (Shannon et al., 2003).Meta-analysis: We performed meta-analysis as described before (Langfelder et al., 2016; Zaykin, 2011).

For each protein i and dataset a, we calculated a Z statistic Z_{ia}: $Z = p / \sqrt{n}$

Then the meta-analysis Z_i score for each protein was calculated as:

$$Z_i = \frac{1}{\sqrt{N_{\text{sets}}}} \sum_{a=1}^{N_{\text{sets}}} Z_{ia}$$

Next, the corresponding *p* values were derived via Gaussian distribution using the Z_i scores.

Affinity purification of AMPA receptor complexes

We leveraged our previously described protocol that was originally used for single-particle EM study of native AMPA-Rs (Nakagawa et al., 2005). Briefly, an anti-GluA2CT antibody conjugated to ProteinA sepharose beads to purified native AMPA-R complexes from CHAPS extracted brain membrane obtained from 15 PDAPP J20 or non-transgenic litter mate brains (lacking cerebellum) of mixed ages from 3 – 12 months of age. Beads conjugated with normal rabbit IgG were prepared similarly and used during purification as negative control. Mouse brains were homogenized in 20 mM HEPES, pH 7.4, 320 mM sucrose, 5 mM EDTA, 5 mM EGTA, 30 uM NBQX supplemented with protease inhibitors (1 mM PMSF, 10 ug/ml aprotinin, 10 ug/ml leupetin, 1 ug/ml pepstatin, and 500 uM benzamidine). Supernatant was obtained by centrifuging the homogenate at 3,000 g for 15 min was further spun at 38,400 g for 15 min to obtain a membrane pellet (P2 fraction). P2 was resuspended in SB1 (20 mM HEPES, pH 7.4, 1 M KI, 5 mM EDTA, 5 mM EGTA, and 30 uM NBQX) and membranes were collected by centrifugation. Membranes were further washed with WB (20 mM HEPES, pH 7.4, 5 mM EDTA, 5 mM EGTA, 30 mM NBQX) to remove KI. Finally, membranes were solublized in RB (20 mM HEPES, pH 7.4, 100 mM NaCl, 5 mM EDTA, 5 mM EGTA, 1 % CHAPS, 30 uM NBQX, with protease inhibitors) for 3 hr with gentle stirring at 4 ^{o}C and ultracentrifuged at 100,000 g to remove insoluble material. The final supernatant was applied to appropriate antibody affinity column (0.25 ml bed volume, antibody concentration 2 mg/ml). After washing the column with 3 ml of sample buffer, bound proteins were eluted with 100 mM glycine pH 2.5, 1% CHAPS and each eluted fractions were immediately mixed with 1/10 volume of 1M TrisHCl pH8.5. The column elution was conducted using 20 mM HEPES, pH 7.4, 150 mM NaCl, 5 mM EDTA, 5 mM EGTA, 1% CHAPS, 30 uM NBQX, 0.5 μg / ml GluA2 C-terminal epitope peptide (GYNVYGIESVKI). The affinity purified material was then precipitated with 15% TCA (trichloroacetic acid). Purified proteins processed and analyzed as described above. For each purification (both mouse and human) we normalized the level of each AMPAR subunit recovered relative to the immunoprecipitated GluA2 protein based on spectral counts.

Electrophysiology

After removal, the brains of hAPP-J9 (field recordings, Fig. S5) or hAPP-J20 (whole-cell voltage clamp recordings, Fig. 7) were placed in ice-cold carbogenated artificial cerebrospinal fluid (ACSF) containing 83 mM NaCl, 2.5 mM KCl, 1 mM NaH_2PO4, 26.2 mM NaHCO3, 22 mM glucose, 72 mM sucrose, 0.5 CaCl2, and 3.3 mM $MgSO_4$. After cutting 300 μm sagittal sections on a Leica VT1200 vibratome, slices recovered at 31°C for 40 min and then at room temperature for 30 min to 6 hr. Slices were then placed in carbogenated recording ACSF (119 mM NaCl, 2.5 mM KCl, 26 mM NaHCO3, 1 mM NaH2PO4, 1.5 mM MgSO4, 2.5 mM CaCl2, and 11 mM glucose) that contained 100 μM picrotoxin (Tocris). In most experiments, a small cut was made to separate CA3 from CA1 to prevent recurrent excitation from contaminating the recording. Signals were recorded with a 5× gain, low-pass filtered at 2 kHz and digitized at 10 kHz (Molecular Devices Multiclamp 700B) and analyzed with pClamp 10 (Molecular Devices). Whole-cell recordings were made using 3–5 MΩ pipettes filled with an internal solution that contained 123 mM Cs-gluconate, 8 mM NaCl, 1 mM CaCl2, 10 mM EGTA, 10 mM HEPES, and 10 mM glucose, pH 7.3 with CsOH, 280–290 mOsm. Series resistance (Rs) and input resistance (Rin) were monitored throughout the experiment by measuring the capacitive transient and steady-state deflection in response to a −5mV test pulse, respectively. Cells were excluded if Rs varied by more than 20% during a recording. Field recordings were obtained using a 1–2 MΩ pipette filled with ACSF. Responses were evoked by stimulating axons in the stratum radiatum with a platinum 2-contact cluster electrode (FHC) 100-200 microns lateral to the recording site. For fEPSP and whole cell voltage clamp experiments, analysis was usually based on the average of 15 sweeps. CA1 pyramidal cells were visualized by infrared differential interference microscopy (Olympus BX51WI). To measure AMPAR-mediated currents, cells were voltage clamped at -70mV and the peak response was measured. To measure the NMDAR-mediated current, cells were depolarized to +40mV and analyzed as the mean of a 10 ms window beginning 50ms after the stimulus artifact, by which time the fast AMPA component had decayed and the remaining response could be attributed to NMDAR-mediated currents. Summary statistics represent mean ± SEM.

Purification of AMPA-R from human brain

Human brain (cortex) was obtained through the National Disease Research Interchange (NDRI), Researcher: Yates (code YAJ2), TSRI: IRB-11-5719. The antigen of the antibody against GluA2 is conserved in rat and human. GluA2 from human cortex was immunoaffinity purified using identical purification protocol used to purify rat GluA2. In general, we used 20g of brain tissue as the input material for our AMPA receptor complex purifications, but in two experiments we used 160 g and 195 g.

NDRI #	Normal / Diseased	Brain region	Cause of death	Gender	Age	Hours post	Year of death
67325	Normal	Cortex	Heart Failure	F	85	8.1	2011
67327	Normal	Cortex	Kidney Cancer with mets	M	85	5.1	2011

67629	Diseased	Cortex	Alzheimer's disease	F	-	6.5	2011
67402	Diseased	Cortex	Alzheimer's disease	F	86	9.9	2011
67728	Diseased	Cortex	Alzheimer's disease	F	78	11	2011
67402	Diseased	Cortex	Alzheimer's disease	F	86	9.9	2011

SUPPLEMENTAL REFERENCES

Benjamini, Y., and Hochberg, Y. (1995). Controlling the False Discovery Rate - a Practical and Powerful Approach to Multiple Testing. J Roy Stat Soc B Met *57*, 289-300.

Blum, T., Briesemeister, S., and Kohlbacher, O. (2009). MultiLoc2: integrating phylogeny and Gene Ontology terms improves subcellular protein localization prediction. BMC Bioinformatics *10*, 274.

Cociorva, D., D, L.T., and Yates, J.R. (2007). Validation of tandem mass spectrometry database search results using DTASelect. Curr Protoc Bioinformatics *Chapter 13*, Unit 13 14.

Cohen, E., Paulsson, J.F., Blinder, P., Burstyn-Cohen, T., Du, D., Estepa, G., Adame, A., Pham, H.M., Holzenberger, M., Kelly, J.W., *et al.* (2009). Reduced IGF-1 signaling delays age-associated proteotoxicity in mice. Cell *139*, 1157-1169.

Elias, J.E., and Gygi, S.P. (2007). Target-decoy search strategy for increased confidence in large-scale protein identifications by mass spectrometry. Nat Methods *4*, 207-214.

Eng, J.K., Mccormack, A.L., and Yates, J.R. (1994). An Approach to Correlate Tandem Mass-Spectral Data of Peptides with Amino-Acid-Sequences in a Protein Database. J Am Soc Mass Spectr *5*, 976-989.

Fabregat, A., Sidiropoulos, K., Garapati, P., Gillespie, M., Hausmann, K., Haw, R., Jassal, B., Jupe, S., Korninger, F., McKay, S., *et al.* (2016). The Reactome pathway Knowledgebase. Nucleic Acids Res *44*, D481-487.

Langfelder, P., and Horvath, S. (2008). WGCNA: an R package for weighted correlation network analysis. BMC Bioinformatics *9*, 559.

Lavallee-Adam, M., Rauniyar, N., McClatchy, D.B., and Yates, J.R., 3rd (2014). PSEA-Quant: a protein set enrichment analysis on label-free and label-based protein quantification data. J Proteome Res *13*, 5496-5509.

Link, A.J., Eng, J., Schieltz, D.M., Carmack, E., Mize, G.J., Morris, D.R., Garvik, B.M., and Yates, J.R., 3rd (1999). Direct analysis of protein complexes using mass spectrometry. Nat Biotechnol *17*, 676-682.

Ly, P.T.T., Cai, F., and Song, W.H. (2011). Detection of Neuritic Plaques in Alzheimer's Disease Mouse Model. Jove-J Vis Exp.

MacCoss, M.J., Wu, C.C., Liu, H., Sadygov, R., and Yates, J.R., 3rd (2003). A correlation algorithm for the automated quantitative analysis of shotgun proteomics data. Anal Chem *75*, 6912-6921.

MacCoss, M.J., Wu, C.C., Matthews, D.E., and Yates, J.R., 3rd (2005). Measurement of the isotope enrichment of stable isotope-labeled proteins using high-resolution mass spectra of peptides. Anal Chem *77*, 7646-7653.

McDonald, W.H., Tabb, D.L., Sadygov, R.G., MacCoss, M.J., Venable, J., Graumann, J., Johnson, J.R., Cociorva, D., and Yates, J.R., 3rd (2004). MS1, MS2, and SQT-three unified, compact, and easily parsed file formats for the storage of shotgun proteomic spectra and identifications. Rapid Commun Mass Spectrom *18*, 2162-2168.

Nakagawa, T., Cheng, Y., Ramm, E., Sheng, M., and Walz, T. (2005). Structure and different conformational states of native AMPA receptor complexes. Nature *433*, 545-549.

Savas, J.N., De Wit, J., Comoletti, D., Zemla, R., Ghosh, A., and Yates, J.R., 3rd (2014). Ecto-Fc MS identifies ligand-receptor interactions through extracellular domain Fc fusion protein baits and shotgun proteomic analysis. Nat Protoc *9*, 2061-2074.

Savas, J.N., Toyama, B.H., Xu, T., Yates, J.R., 3rd, and Hetzer, M.W. (2012). Extremely long-lived nuclear pore proteins in the rat brain. Science *335*, 942.

Shannon, P., Markiel, A., Ozier, O., Baliga, N.S., Wang, J.T., Ramage, D., Amin, N., Schwikowski, B., and Ideker, T. (2003). Cytoscape: a software environment for integrated models of biomolecular interaction networks. Genome Res *13*, 2498-2504.

Soriano, S., Lu, D.C., Chandra, S., Pietrzik, C.U., and Koo, E.H. (2001). The amyloidogenic pathway of amyloid precursor protein (APP) is independent of its cleavage by caspases. J Biol Chem *276*, 29045-29050.

Tabb, D.L., McDonald, W.H., and Yates, J.R., 3rd (2002). DTASelect and Contrast: tools for assembling and comparing protein identifications from shotgun proteomics. J Proteome Res *1*, 21-26.

von Mering, C., Jensen, L.J., Snel, B., Hooper, S.D., Krupp, M., Foglierini, M., Jouffre, N., Huynen, M.A., and Bork, P. (2005). STRING: known and predicted protein-protein associations, integrated and transferred across organisms. Nucleic Acids Res *33*, D433-437.

Washburn, M.P., Wolters, D., and Yates, J.R., 3rd (2001). Large-scale analysis of the yeast proteome by multidimensional protein identification technology. Nat Biotechnol *19*, 242-247.

Xu, T., Park, S.K., Venable, J.D., Wohlschlegel, J.A., Diedrich, J.K., Cociorva, D., Lu, B., Liao, L., Hewel, J., Han, X., *et al.* (2015). ProLuCID: An improved SEQUEST-like algorithm with enhanced sensitivity and specificity. J Proteomics *129*, 16-24.
Zaykin, D.V. (2011). Optimally weighted Z-test is a powerful method for combining probabilities in meta-analysis. J Evol Biol *24*, 1836-1841.